sciendo
ISSN 1335-8871
MEASUREMENT SCIENCE REVIEW
Journal homepage: https://content.sciendo.com

A Virtual Measurement Method of the Transmission Error Based on Point Clouds of the Gear

Bo Yu, Hanlin Kou, Zhaoyao Shi, Yanqiang Sun

Beijing Engineering Research Center of Precision Measurement Technology and Instruments, Faculty of Materials and Manufacturing, Beijing University of Technology, Beijing, China, dr_yubo@126.com

As the most widely used gear measuring instrument, the gear measuring center can measure the individual deviations of a gear tooth flank other than the comprehensive deviations of the gear. However, gear transmission error is an important transmission performance indicator in the gear meshing process. It is an important trend of gear measuring to obtain the transmission error from individual deviations. In this study, a calculation method of gear transmission error is proposed based on the point clouds of the gear obtained by optical sensors. According to the gear meshing principle, a method is introduced to determine the contact status between the tooth flanks formed by the point clouds. According to this introduced method, the single tooth pair meshing process and the meshing process of multiple tooth pairs are analyzed to determine the gear transmission error curve. The comparison results of tooth contact analysis and gear measurement experiments verify the proposed virtual measurement method.

Keywords: Gear measurement, virtual measurement, transmission error, point clouds.

1. INTRODUCTION

As the core part of mechanical products, gears are widely used in aerospace, high-speed trains, automobiles, and robots. Modern machines require gear products with high transmission performance, especially in the field of electric vehicles. Due to simplified automobile transmissions and the extensive application of electric motors replacing engines, gear transmission noise has become the main noise source of electric vehicles [1]. Transmission error (TE) is closely related to the gear transmission noise [2]-[5]. Through the analysis of transmission error, the source of the transmission noise can be further determined. In addition, the transmission error is also correlated with the individual deviations of gears, which indicate the accuracy of gears [6], [7]. Therefore, TE is the hotspot in the gear study.

The transmission error measurement of cylindrical gears is a basic technology to study TE. The traditional TE measurement method is implemented with a single flank tester [8]-[10]. This method is applicable to medium-module gears. For large gears, it is difficult to find the benchmark of gears due to their large volume, mass, and inertia. Small gears have small size, inertia, and stiffness and are easy to deform. In addition, the spindle system of the single flank tester has a large inertia and small gears are not easy to be damped on the tester. Therefore, it is difficult to measure TE of large gears and small gears with high precision. In addition, since the contact ratio of the gears is larger than 1, the measurement results of single flank tester cannot be used to analyze the influence of individual tooth flank deviations on TE.

Besides the single flank tester, the gear integrated error measuring instrument can also be used to measure TE [12]. With this instrument, the unit curves of the gear integrated error of each tooth can be obtained by meshing with the standard tooth-skipped worm with the gear [13], [14]. The envelope of all the unit curves of the gear integrated error is the TE curve. With this measuring instrument, both individual deviations and TE can be acquired. However, it has the same problem with the single flank tester and is not suitable to measure large gears and small gears. This method can only measure one cross-section after every several rotations. In order to obtain all the information of the gear, multiple sections should be measured [15]. The measurement efficiency of this method should be improved.

Direct measurement is an effective method to acquire TE. In addition, TE can also be calculated with the gear tooth flank model. In the most common method, the meshing equation is used based on the meshing principle [16], [17]. However, before the application of this method, the models of two tooth flanks should be known, so it is only applicable to continuous conjugated tooth surfaces. For tooth flanks formed by discrete point clouds, other mathematical methods should be considered. At present, the gear measuring center is the most widely used instrument for measuring gears. By scanning the discrete data points of the tooth flank, it can

DOI: 10.2478/msr-2022-0012

measure individual deviations such as profile deviation, helix deviation, and pitch deviation [18], [19]. TE of gears can be obtained from individual deviations so as to realize the measurement of TE of large gears and small gears. However, the gear measurement center only acquires partial information of the gear [20]. There is a difference between actual TE and the TE calculated with these data points.

In this study, a virtual measurement method of cylindrical gear transmission error is proposed based on the point clouds of tooth flanks measured by the optical approach. In the proposed method, point clouds are directly used to establish the model of the gear and calculate TE. The proposed method can replace the traditional TE measuring method. This method is applicable to most cylindrical gears. Based on the point clouds of the tooth flanks obtained with the optical approach, it can be applied in rapid on-line testing of automobile gears to obtain individual deviations and TE of gears. It is of great significance to the analysis of transmission noise.

2. VIRTUAL MEASUREMENT PROCESS OF TE OF CYLINDRICAL GEARS

The virtual measurement method of the transmission error of cylindrical gears is established on the basis of the point clouds of tooth flanks, as shown in Fig.1.

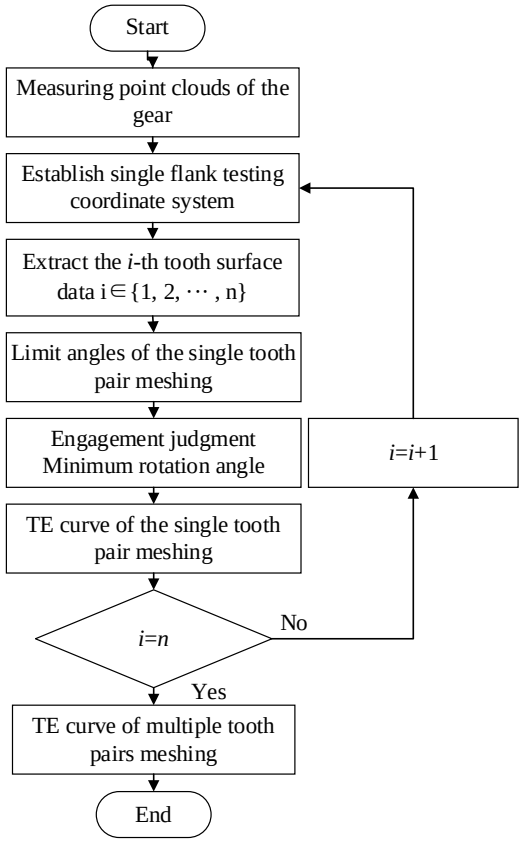

Fig.1. Flow chart of virtual measurement.

First, the gear measuring center is used to obtain point clouds of tooth flanks. This process can use the traditional contact probe, but the measured data points are not enough to describe the meshing characteristics of the whole tooth flank. The optical measurement approach can obtain more complete information of tooth flanks and is more suitable for this process. $\vec{P}_{ijk}$ is used to represent the point clouds of the measured gear, which are composed of several layers of data points. i represents the sequence number of the tooth flank, $i \in \{1, 2, \cdots, n\}$. k represents the layer sequence number of the data points on the current tooth flank, $k \in \{1, 2, \cdots, m\}$. j represents the sequence number of the data point in the current layer, $j \in \{1, 2, \cdots, q\}$. n is the number of measured gear teeth. m is the number of the layers of point clouds and q is the number of the points in each layer.

Then, the measurement coordinate system of the single flank testing is established and the data points of the *i*-th tooth flank are extracted from the point clouds of the whole measured gear. According to the spatial relationship between the measured gear and the master gear, the limit angles of the meshing process of the single tooth pair are determined. The meshing process includes the engaging-in tip meshing process, normal meshing process, and engaging-out tip meshing process [14]. In the range of the limit angle, the minimum rotation angle of the master gear is used to determine the meshing status of the discrete tooth flank at each angle of the measured tooth flank. The minimum rotation angle is the angle of the master gear when it meshes with the measured gear. According to the single flank composite deviation calculation method, the TE curve of the single tooth flank can be obtained. Through changing the sequence number of the tooth flank involved in the meshing until $i = n$, it is easy to acquire the TE curves of different tooth flanks.

As the initial position of each tooth flank is different, the rotation angle of each tooth flank to the meshing zone is also different. With the rotation angle as the abscissa and TE as the ordinate, a coordinate system is established. All the TE curves of the tooth flanks are placed in the same coordinate system. Since the contact ratio of the gear is bigger than 1, the zones where the curves overlap are the double-engagement zones, whereas other zones are the single-engagement zones. The TE curve of the whole gear can be obtained with the envelope of the curves.

3. MODEL OF TRANSMISSION ERROR OF A CYLINDRICAL GEAR

Fig.3. shows the virtual measurement method of TE. The calculation method of TE is introduced below. First, the point clouds are divided into *n* flanks. On each flank, they are divided into *m* layers and there are *q* points on each layer. Second, TE of each single flank pair is calculated with the minimum rotation angle method. At last, TE of each single flank pair is combined together to form the TE curve of the gear.

3.1. Single flank testing coordinate system

Virtual measurement is achieved with imaginary gears for single flank testing. It involves two cylindrical gears. One is a master gear as the theoretical gear, the other is a gear composed of point clouds as the measured gear.

As shown in Fig.2., $S_1(O_1;x_1,y_1,z_1)$ is the coordinate system of the master gear and rotates with the master gear. Point O_1 is the origin of $S_1(O_1;x_1,y_1,z_1)$. $S_2(O_2;x_2,y_2,z_2)$ is the coordinate system of the measured gear and rotates with the measured gear. Point O_2 is the origin of $S_2(O_2;x_2,y_2,z_2)$. The axis z_1 is collinear with the axis of the master gear and the axis z_2 is collinear with the axis of the measured gear. The surface $x_1O_1y_1$ and the surface $x_2O_2y_2$ are on the same plane and the axis x_1 and the axis x_2 are in the same straight line. O_1 O_2 is the center distance between the two gears.

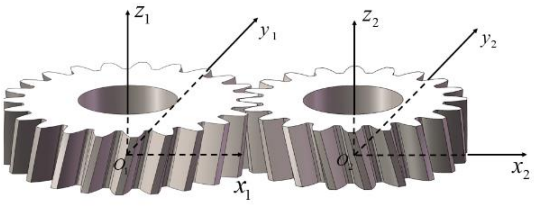

Fig.2. Coordinate system of single flank testing.

3.2. Analysis of the single tooth pair meshing

As shown in Fig.3., Σ_1 is the theoretical tooth flank and Σ_{2i} is the tooth flank when the i-th tooth of the measured gear is rotated clockwise by angle φ_2. Point B is any point of the tooth flank in the coordinate system S_2 and the vector of Point B is $\vec{P}_{ijk}$. Plane C is a transverse section passing Point B. L_1 is the theoretical gear tooth profile on Plane C and L_2 is the tooth profile formed by the point clouds of the measured gear on Plane C. The vector set of tooth profile L_2 is:

$$L_2 := \left\{ \vec{P}_{ijk} \middle| i = i_B,\ k = k_B,\ j \in \{1, 2, \cdots, q\} \right\} \tag{1}$$

where i_B is the sequence number of the current tooth on which Point B is; k_B is the sequence number of the current layer on which Point B is.

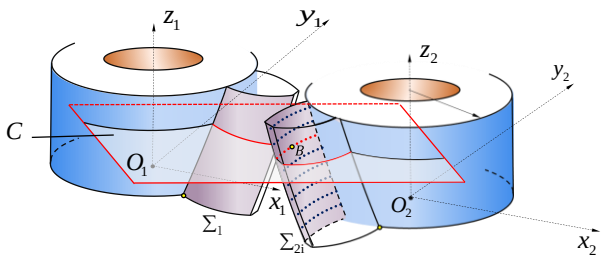

Fig.3. Single tooth pair meshing.

In order to facilitate the analysis of the meshing process in Plane C, the plane is extracted, as shown in Fig.4. R_1 and R_2 are the reference radii of the theoretical gear and the measured gear, respectively. The current rotation angle of L_2 is φ_2. $\vec{r}_B$ is the vector of Point B in the coordinate system S_1.

$$\vec{r}_B = M_{12}\vec{P}_{ijk} \tag{2}$$

where M_{12} is the transformation matrix from the coordinate system S_2 to S_1. If L_1 meshes with L_2 at Point A, the vector $\vec{r}_A$ of Point A is expressed as:

$$\vec{r}_A = \vec{r}_B . \tag{3}$$

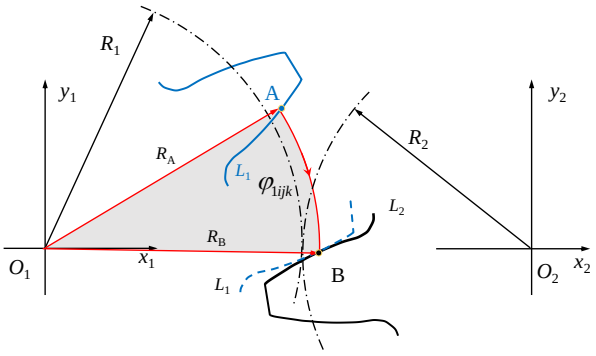

Fig.4. Tooth profiles on Plane *C*.

According to the forming principle of the involute helicoid, the tooth flank model is established as follows [21]:

$$\vec{r}_A = \vec{r}_A(u_1, \theta_1, \varphi_1) \tag{4}$$

where u_1 is the parameter along the axis; θ_1 is the parameter along the tooth profile; φ_1 is the rotation angle of the theoretical gear. According to the contact condition of the two tooth flanks, equation (5) can be established and the coordinates of Point A in S_1 can be determined.

$$\begin{cases} \vec{r}_A = \vec{r}_A(u_1, \theta_1, \varphi_1) \\ \vec{r}_A = \vec{r}_B \end{cases} \tag{5}$$

Equations (1) to (5) demonstrate the calculation process of the rotation angle φ_{1ijk} of L_1 when Σ_1 and Σ_{2i} are in contact at Point B. There are q points on L_2. As φ_2 of Σ_{2i} is constant for the moment, all data points on L_2 are processed according to the above process so that a rotation angle φ_{1ijk} of L_1 at each point on L_2 is acquired. Minimum value of φ_{1ijk} determines the status that L_1 meshes with L_2 on this plane and is expressed as:

$$\varphi_{1ik} = \min\{\varphi_{1ijk}\} \quad i = i_1, k = k_B,\ j \in \{1, 2, \cdots, q\} \tag{6}$$

This process is to judge the meshing point on one layer. There are m layers on the Σ_{2i}. For each layer, φ_{1ik} can be

calculated with equation (6). The minimum value of φ_{1ik} determines the status that Σ_1 and Σ_{2i} are engaged with each other. The new minimum value is expressed as:

$$\varphi_{1i} = \min\{\varphi_{1ik}\} \quad i = i_1, k \in \{1, 2, \cdots, m\} \tag{7}$$

When φ_2 is changed to a new value, a new φ_{1i} of Σ_1 is acquired through the above process.

In the meshing process, a single tooth flank goes through three stages: the engaging-in tip meshing stage in which the tooth tip of the driven gear slides on the tooth flank of the driving gear, the normal tooth profile meshing stage, and the engaging-out tip meshing stage in which the tooth tip of the driving gear slides on the tooth flank of the driven gear [14]. Therefore, the limit angles of the single tooth pair meshing are determined with the tip circles of the driving gear and the driven gear. In Fig.5., Point *M* and Point *N* are the intersection points of the two tip circles. The two points are the limit positions of the single tooth pair meshing.

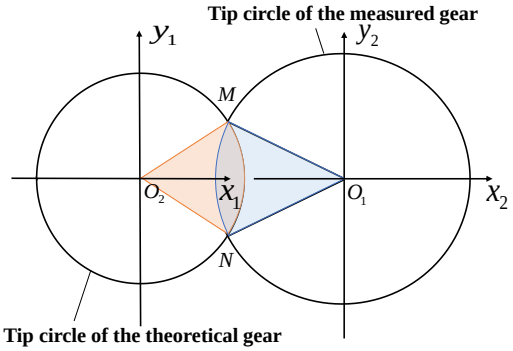

Fig.5. Limit positions of the single tooth pair meshing.

In the range of the limit angles of the single tooth pair meshing, the meshing process of the whole tooth flank Σ_{2i} can be analyzed by changing the rotation angle φ_2 of the measured gear. If φ_2 varies from the engage-in stage to the engage-out stage (Position *N* to Position *M* in Fig.5.), a group of φ_{1i} one to one corresponding to φ_2 are determined. In this way, TE of one single tooth pair can be calculated as:

$$TE = \left[\varphi_2 - \left(\frac{Z_1}{Z_2}\right)\varphi_{1i}\right] \times r_{b2} \tag{8}$$

where Z_1 and Z_2 are the numbers of the teeth of the theoretical gear and the measured gear, respectively; r_{b2} is the radius of the basic circle of the measured gear.

With TE as the vertical axis and φ_2 as the horizontal axis, the TE curve of single tooth pair meshing is plotted in Fig.6.

3.3. *Analysis of multiple tooth pair meshing*

After the single tooth pair meshing process analysis in Section 3.2 is carried out for all tooth flanks, TE can be obtained. As the initial position of each tooth flank is different, the rotation angle of each tooth flank to the meshing zone is different. TE data of all tooth flanks are plotted in the same coordinate system to form the red curve shown in Fig.3. In the coordinate system, the abscissa is the rotation angle of each tooth flank and the ordinate is TE at a corresponding angle. As the contact ratio of gears is larger than 1, the overlapping zone exists in the TE curves of two adjacent tooth flanks. With the formed envelope of the curves, the TE curve of the entire gear can be obtained as the black curve shown in Fig.6.

$$TE = \begin{cases} TE_i & when\ TE_i \geq TE_{i+1} \\ TE_{i+1} & when\ TE_i < TE_{i+1} \end{cases} \tag{9}$$
$$i \in \{1, 2, \cdots, n\},\ when\ i = n,\ TE_{i+1} = TE_1$$

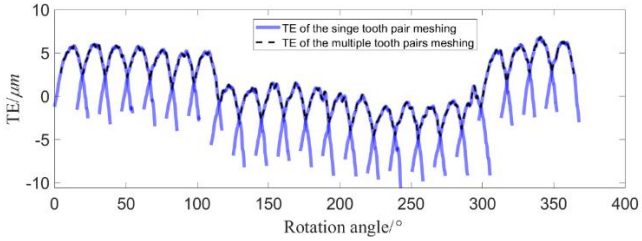

Fig.6. TE curve of multiple tooth pair meshing.

4. COMPARISON WITH TOOTH CONTACT ANALYSIS RESULTS

To verify the proposed method, the calculation results obtained with simulation data are compared with the results of the traditional tooth contact analysis (TCA). In TCA, continuous tooth flanks are used to calculate the meshing model. This method deals with the discrete simulated tooth flank. In this section, TE obtained from the single tooth pair meshing analysis is verified. The multiple tooth pair meshing analysis is verified by the measurement experiments in Section 5.

4.1. *Parameters of gears*

The parameters of the tested gear and the master gear for the simulation are shown in Table 1.

Table 1. Parameters of the simulated gears.

Parameters	Master Gear	Tested Gear
Number of teeth	42	42
Module / *mm*	3	3
Pressure angle /°	20	20
Tip diameter / *mm*	132	132
Root diameter / *mm*	124.5	124.5
Facewidth / *mm*	6	6

To show the influence of the tooth profile deviation on TE better, crowned errors are superimposed in the normal direction of the tooth profile. The maximum crowned error is 0.1 *mm*. In Fig.7., the blue line is the theoretical tooth profile and the black line is the tooth profile with errors.

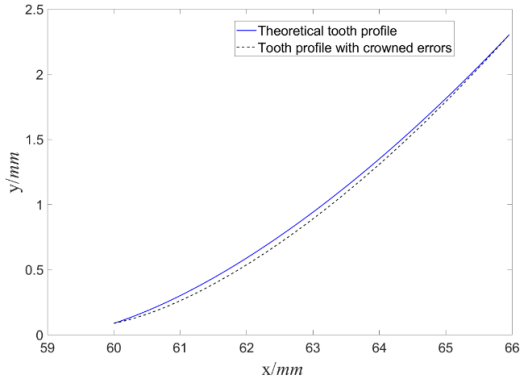

Fig.7. Simulated tooth profile.

4.2. *Comparison of simulation results*

In Fig.8., TE calculated by TCA is marked as the black line and that of the proposed method is marked as the blue line.

Since the TE curves calculated with the two methods are similar, the difference cannot be directly observed from Fig.8. The difference between the two TE curves is shown in Fig.9.

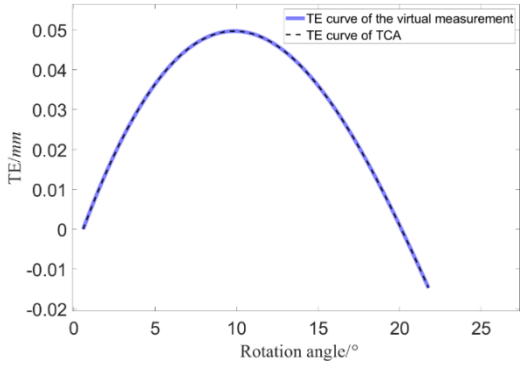

Fig.8. Comparison of TE curves of virtual measurement and TCA.

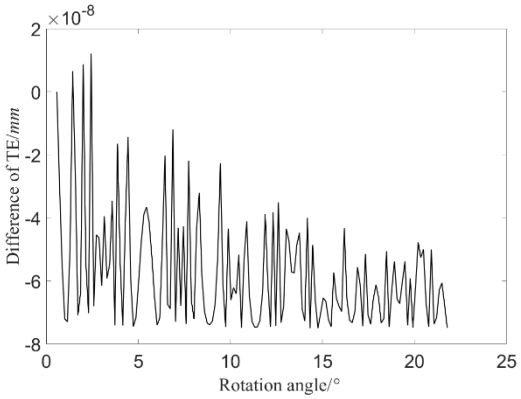

Fig.9. Differences between TE curves of the two methods.

The result calculated by a computer is the numerical solution, indicating that an error exists depending on the solver. The accuracy in this case is limited to the order of magnitude, 10^{-11} *mm*.

Fig.9. illustrates that the difference of TE calculated by the two methods is about 10^{-8} *mm*. The small error is interpreted as follows. The number of discrete points is limited and the discrete points are used to replace the surface around them in the calculation, thus leading the loss of partial surface information. Therefore, the denser the discrete points are, the smaller the difference is.

During gear measurement, TE of the gear is usually 10^{-2}~10^{-3} *mm* [22]. The accuracy of this method is determined by the density of the point clouds. The error in the case of this section is 10^{-8} *mm*, which is far less than the measured deviation. Therefore, the principle error of this method can be ignored.

5. EXPERIMENTS AND DISCUSSION

5.1. *Instruments*

5.1.1. *Measurement of the point clouds of the gear*

The gear measuring center equipped with a line-structured laser sensor was used to obtain the point clouds on the surface of the gear. As shown in Fig.10., the measuring instrument is composed of a line-structured laser sensor, a fixture, a rotating platform, 3-D moving platform, and a measured gear. Through the movement of the 3-D platform, the position of the line-structured laser sensor can be adjusted to measure gears of different sizes. The measuring curve of the line-structured laser sensor is composed of 800 points and the measuring repeatability can reach 0.5 μm. The accuracy of the rotating platform is ±5″.

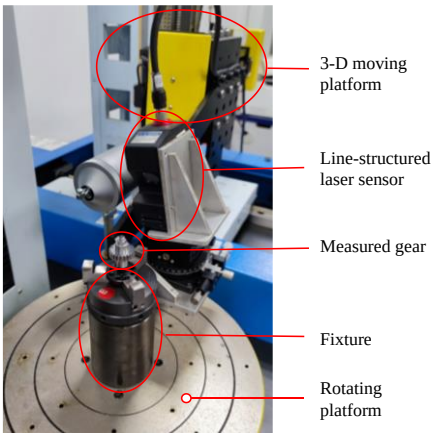

Fig.10. Measuring instrument of the point clouds of the gear.

5.1.2. *Measurement of TE*

To verify whether the virtual measurement method proposed in this paper can replace the actual measurement method, the results of this method are compared with the results measured by the single flank tester. As shown in Fig.11., it is mainly composed of a servo motor, two circular gratings, a torque sensor, and a hysteresis brake. The input part can move along the center distance direction to adjust the center distance between the master gear and the measured gear. The output part can move along the gear axis. By adjusting the center distance and the axial distance, the instrument can be adapted to the measurement of gears with different parameters. The measuring repeatability of the instrument is ±2 μm.

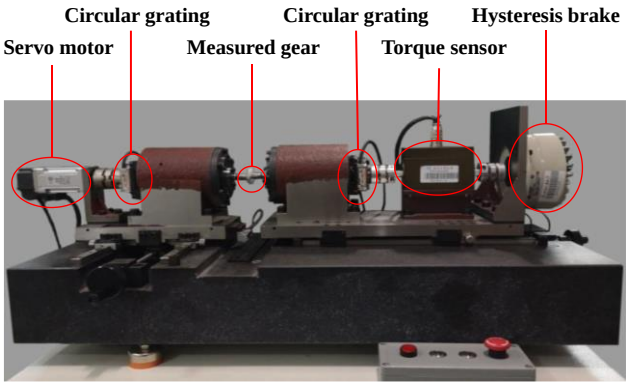

Fig.11. Single flank tester.

5.2. Parameters of the measured gears

Table 2. shows the parameters of the measured gears. Gear 1 is a gear with a crowned modification. Gear 2 has a negative pressure angle error, whereas Gear 3 has a positive pressure angle error.

Table 2. Parameters of measured gears.

Parameters	Master gear	Gear 1	Gear 2	Gear 3
Number of teeth	38	23	23	23
Module / *mm*	1	1	1	1
Pressure angle / °	20	20	19	21
Tip diameter / *mm*	40	25	25	25
Root diameter / *mm*	35.5	20.5	20.5	20.5
Facewidth / *mm*	13	6	6	6
Modification	None	Crowned	None	None

5.3. Measured results

5.3.1. Measured results from the point clouds of the gears

The angle signal of the rotating platform is used as an external trigger source to synchronously trigger the line-structured laser sensor for data acquisition. The line-structured laser sensor performs one acquisition every 0.01° that the platform rotates. When the measured gear rotates a round with the rotating platform, the line-structured laser sensor scans the gear surface. In this way, the point clouds of the gear can be obtained. Fig.12. shows the point clouds of the gear. The errors are small and it is difficult to observe the differences among the point clouds of the three gears.

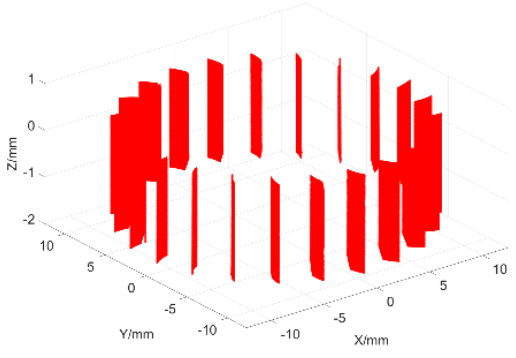

Fig.12. Point clouds of the measured gears.

According to the method proposed in this study, TE curves are derived from the point clouds of three gears. The calculation results are shown as red lines in Fig.13.

5.3.2. Measured results from the single flank tester

The driving gear was a master gear and the driven gear was a measured gear. When the driven gear rotated from 0° to 360°, the rotation angles of the driving gear and the driven gear were recorded. The measured curves of the TE of Gear 1, Gear 2, and Gear 3 are shown as the black lines in Fig.13.

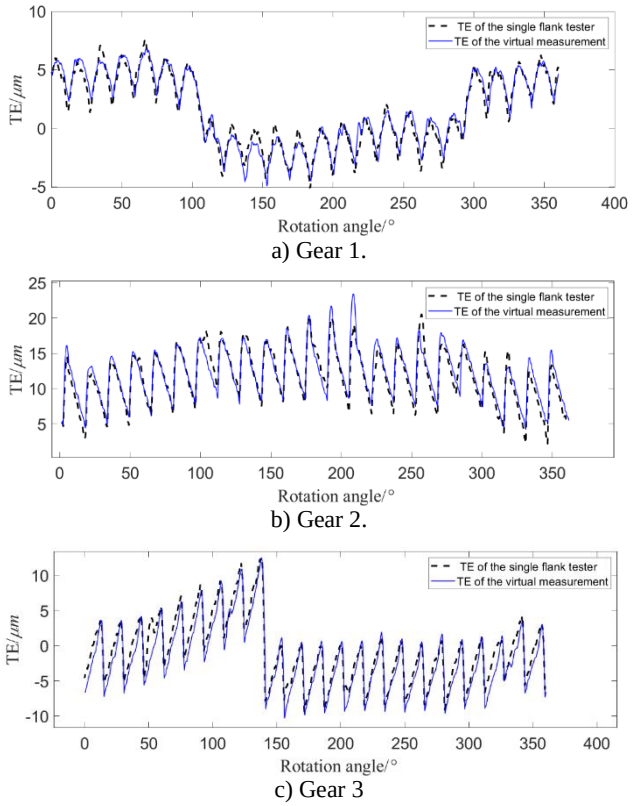

a) Gear 1.

b) Gear 2.

c) Gear 3

Fig.13. Comparison of the results of the virtual measurement and the single flank tester for Gear 3.

5.4. Discussion

To compare the results of the virtual measurement and the single flank tester more clearly, the curves are plotted in Fig.13.

5.4.1. Analysis of Gear 1

The crowned modification on the tooth profile of Gear 1 is directly mapped to TE. In Fig.13.a), the curve is a crowned shape in the single tooth pair meshing period. The number of single tooth meshing pair periods of the virtual measurement is the same as that of the measured curve. The differences between adjacent periods for two curves are similar, indicating that the pitch deviations of them are nearly the same. In a single tooth pair meshing cycle, the engage-in stages and the engage-out stages of the two curves both overlap well. In the middle stage, some parts overlap well, but other parts show the difference of 1~2 *μm*.

According to the definition in ISO1328 [22], the tooth-to-tooth single flank composite deviation and the total single flank composite deviation are calculated with the data in Fig.13.a). The calculation results are provided in Table 3. The differences between the single flank composite deviations of the virtual measurement and the actual measurement are less than 1 μm.

Table 3. Single flank composite deviations of Gear 1.

Items	Tooth-to-tooth single flank composite deviation / μm	Total single flank composite deviation / μm
Virtual measurement	6.58	11.76
Actual measurement	6.74	12.54
Differences	-0.16	-0.78

5.4.2. Analysis of Gear 2

The tooth profile of Gear 2 has a negative pressure angle error. In the engage-in stage, the negative pressure angle error leads to the tip meshing stage. TE decreases linearly in the normal tooth profile meshing stage. There are tip meshing stages in which the curves are steep (Fig.13.b)). Then, the normal meshing stage starts and TE decreases linearly.

The tooth-to-tooth single flank composite deviation and the total single flank composite deviation are calculated with the data in Fig.13.b). The calculation results are provided in Table 4. The differences between the single flank composite deviations of the virtual measurement and the actual measurement are less than 2 μm.

Table 4. Single flank composite deviations of Gear 2.

Items	Tooth-to-tooth single flank composite deviation / μm	Total single flank composite deviation / μm
Virtual measurement	15.87	19.00
Actual measurement	14.37	17.41
Differences	1.50	1.59

5.4.3. Analysis of Gear 3

The tooth profile of Gear 3 has a positive pressure angle error. In the single tooth pair meshing period, TE of gears with a positive pressure angle error increases linearly in the normal meshing stage. Due to the positive pressure angle errors, the tip meshing stage occurs at the engage-out stage, as shown in Fig.13.c). The single tooth pair meshing period starts with the normal meshing stage in which TE increases linearly. Then it enters the tip meshing stage in which the TE curve is relatively steep. The tip meshing stage is determined by the tip of the master gear. As the deviation of the master gear is small and the transition between the tip and the flank is smooth, TE data of the virtual measurement and the actual measurement are almost the same in the tip meshing stage.

The tooth-to-tooth single flank composite deviation and the total single flank composite deviation are calculated with the data in Fig.13.c). The calculation results are provided in Table 5. The differences between the single flank composite deviations of the virtual measurement and the actual measurement are less than 2 μm.

Table 5. Single flank composite deviations of Gear 3.

Items	Tooth-to-tooth single flank composite deviation / μm	Total single flank composite deviation / μm
Virtual measurement	21.55	22.82
Actual measurement	20.39	21.90
Differences	1.16	0.92

6. CONCLUSIONS

This article proposes a virtual measurement method for measuring TE of cylindrical gears based on point clouds of gears. With this method TE can be directly calculated with point clouds acquired by the gear measuring center equipped with optical sensors. Then, the tooth-to-tooth single flank composite deviation and the total single flank composite deviation can be determined. The calculation results are compared with the single tooth pair meshing process calculated by TCA, proving that the principle error of the virtual measurement method can be ignored. Therefore, the proposed method is correct. Three gears were used in actual measuring experiments and the experimental results were compared with those of the virtual measurement method. Although there were some differences between the results of the virtual measurement and the actual measurement, the TE curves were basically the same in general, indicating that the virtual measurement method could be used to measure TE of gears.

The virtual measurement method facilitates TE measurement because TE can be acquired by the gear measuring center without the single flank tester. When the proposed method is used to measure TE of two gears, the transmission characteristics of the gears can be predicted and utilized in gear pairing.

ACKNOWLEDGMENT

This work was funded by National Key R&D Program of China (2018YFB2001400) and National Natural Science Foundation (52175036).

REFERENCES

[1] Liu, C.Z., Yin, X.S., Liao, Y.H., Yi, Y.Y., Qin D.T. (2020). Hybrid dynamic modeling and analysis of the electric vehicle planetary gear system. *Mechanism and Machine Theory*, 150, 103860. https://doi.org/10.1016/j.mechmachtheory.2020.103860

[2] Smith, J.D. (2003). *Gear Noise and Vibration*. New York: Marcel Dekker.

[3] Smith, R.E. (1986). Identification of gear noise with single flank composite measurement. *Gear Technology*, May/Jun, 17-29.

[4] Smith, R.E. (1988). The relationship of measured gear noise to measured gear transmission errors. *Gear Technology*, Jan/Feb, 38-47.

[5] Palermo, A., Britte, L., Janssens, K., Mundo, D., Desmet, W. (2018). The measurement of Gear Transmission Error as an NVH indicator: Theoretical discussion and industrial application via low-cost digital encoders to an all-electric vehicle gearbox. *Mechanical Systems and Signal Processing*, 110, 368-389. https://10.1016/j.ymssp.2018.03.005

[6] Munro, R.G. (1969). Effect of geometrical errors on the transmission of motion between gears. *Institution of Mechanical Engineers*, 184 (15), 79-84. https://doi.org/10.1243/PIME_CONF_1969_184_445_02

[7] Shi, Z.Y., Kang, Y., Lin, J.C. (2010). Comprehensive dynamics model and dynamic response analysis of a spur gear pair based on gear pair integrated error. *Journal of Mechanical Engineering*, 46 (17), 55-61. https://10.3901/JME.2010.17.055

[8] Munro, R.G. (1979). Review of the single flank method for testing gears. *Annals of CIRP*, 28 (1), 325-329.

[9] Smith, R.E. (2003). Single-flank testing of gears. *Gear Technology*, Mar/Apr, 18-21.

[10] Shi, Z.Y., Ren, X.L., Yu, B., Li, H.Z., Zhang, L.T., Ye, Y., Li, P. (2019). Development of transmission error dynamic testing machine for plastic gear. *Journal of Mechanical Transmission*, 43 (9), 144-147. https://10.16578/j.issn.1004.2539.2019.09.025

[11] Shi, Z.Y., Zhang, W.N., Qu, H.F. (2011). Development of measuring machine based on single-flank testing for fine-pitch gears. *Chinese Journal of Scientific Instrument*, 32 (4), 913-919. https://10.19650/j.cnki.cjsi.2011.04.030

[12] Zhang, Z.L., Huang, T.N., Huang, S.L., Kang, D.Y., Wang, H., Duan, R.G., Xu, L. (1997). A new kind of gear measurement technique. *Measurement Science & Technology*, 8 (7), 715-720. https://doi.org/10.1088/0957-0233/8/7/004

[13] Shi, Z.Y., Wang, X.Y., Shu, Z.H. (2016). Theoretical method for calculating the unit curve of gear integrated error. *Journal of Mechanical Design*, 138 (3), 033301. https://doi.org/10.1115/1.4032400

[14] Shi, Z.Y., Shu, Z.H., Yu, B., Wang, T., Wang X.Y. (2017). Gear reverse-order meshing—phenomenon, analysis, and application. *Journal of Mechanical Design*, 139 (12), 124502. https://doi.org/10.1115/1.4037799

[15] Huang, T.N. (1973). Gear dynamic composite error and its measurement method. *Science in China*, 17 (4), 434-453.

[16] Litvin, F.L., Lu, J., Townsend, D.P., Howkins, M. (1999). Computerized simulation of meshing of conventional helical involute gears and modification of geometry. *Mechanism and Machine Theory*, 34 (1), 123-147. https://doi.org/10.1016/S0094-114X(98)00013-5

[17] Litvin, F.L., Fuentes, A., Gonzalez-Perez, I., Carvenali, L., Kawasaki, K., Handschuh, R.F. (2003). Modified involute helical gears: Computerized design, simulation of meshing and stress analysis. *Computer Methods in Applied Mechanics and Engineering*, 192 (33-34), 3619-3655. https://doi.org/10.1016/S0045-7825(03)00367-0

[18] Goch, G. (2003). Gear metrology. *CIRP Annals - Manufacturing Technology*, 52 (2), 659-695. https://doi.org/10.1016/S0007-8506(07)60209-1

[19] Shi, Z.Y., Lin, H., Lin, J.C., Zhang B. (2013). Current status and trends of large gears metrology. *Journal of Mechanical Engineering*, 49 (10), 35-44. https://10.3901/JME.2013.10.035

[20] Li, H.N., Chen, S.Y., Tang, J.Y., Chen, W.T., Ouyang, H.W. (2019). A novel approach for calculating no-load static transmission error based on measured discrete tooth surfaces. *Mechanism and Machine Theory*, 138, 112-123. https://doi.org/10.1016/j.mechmachtheory.2019.03.044

[21] Yu, B., Shi, Z.Y., Lin, J.C. (2017). Topology modification method based on external tooth-skipped gear honing. *The International Journal of Advanced Manufacturing Technology*, 92 (9), 4561-4570. https://doi.org/10.1007/s00170-017-0463-2

[22] International Organization for Standardization (ISO). (2013). *Cylindrical gears - ISO system of flank tolerance classification - Part 1: Definitions and allowable values of deviations relevant to corresponding flanks of gear teeth*. ISO 1328-1:2013.

Received September 13, 2021
Accepted February 21, 2022